An introduction to quantum interferometry: Young's experiment with fock and coherent states

H. Sanabria
Department of Neurobiology and Anatomy, University of Texas Medical School at Houston, Houston, TX 77030, USA,
e-mail: Hugo.Sanabria@uth.tmc.edu

B.M. Rodríguez-Lara
Facultad de Ingeniería "Arturo Narro Siller", Universidad Autónoma de Tamaulipas, 89 330 Tampico, México,
e-mail: bmlara@uat.edu.mx

Recibido el 31 de julio de 2006; aceptado el 18 de enero de 2007

Quantum interferometry uses the quantum properties of light to surpass the Rayleigh diffraction limit inherent in classical interferometry. We have used Fock and coherent states, which describe the electromagnetic input field, a multi-photon counting apparatus, and an operator-based approach to a multi-slit Young's experiment to present the principles behind quantum interferometry. Our calculations show interference fringes that depend on the wavelength of the source λ, the number of slits in the Young's screen—both characteristics present in the classical scheme—, and the number of photons m, that the measurement apparatus detects. The latter dependence generates an effective de Broglie wavelength, λ/m, a phenomenon that can only be observed by taking advantage of the quantum properties of light.

Keywords: Quantum interferometry; Young experiment; photon states; diffraction limit.

La interferometría cuántica utiliza las propiedades no clásicas de la luz para rebasar el límite de difracción de Rayleigh presente en interferometría clásica. Usando estados de Fock y estados coherentes, que describen el campo electromagnético de la fuente de luz, un detector dependiente del número de fotones presentes en el campo, y una descripción operacional del experimento de Young generalizado a múltiples aperturas, presentamos los principios basicos de interferometría cuántica. Los resultados obtenidos muestran franjas de interferencia que dependen de la longitud de onda de la luz λ, del número de aperturas en la pantalla de Young—ambas características presentes en el caso clásico— y del número de fotones m que puede detectar el aparato de medición. Esta última dependencia genera una longitud de onda efectiva de de Broglie dada por λ/m, un fenómeno que sólo puede ser observado utilizando las propiedades cuánticas de la luz.

Descriptores: Interferometría cuántica; experimento de Young; estados de fotones; límite de difracción.

PACS: 01.40.-d; 03.65.Ta; 42.25.Hz

1. Introduction

In classical optics, light is a transversal electromagnetic wave, and when several coherent light sources interfere, they do so by constructive (additive) or destructive interference; this is known as interferometry. A coherent light source is considered to be the light emitted by many radiative sources that are in phase [1]. In quantum optics, light cannot be treated as a electromagnetic wave alone, and a particle description of light is introduced with the existence of a massless particle, with spin one, called a "photon" [2]. Photons are better described as waves and particles, as stated by the duality principle. However, photons are yet to be fully understood[i]. When one is dealing with such particles, interferometry cannot be described by the superposition of waves, as in classical optics, and a different description of interferometry is required.

Photons are fully based on quantum mechanics, and they represent a "quantum" unit of the electromagnetic field. To tackle the well-known, Young experiment from a quantum perspective, we assume previous knowledge of the quantization of the electromagnetic field. Quantization of the electromagnetic field defines the probability of finding some n quanta of light inside a volume of space as a function of a photon number n; such states of light could be described by Fock or coherent states (for more details see Refs. 4 and 5). Fock states could be considered to be the most particle-like state, while coherent states are more wave-like states. We know that, in the end, classical and quantum mechanical descriptions of the Young's experiment agree when the correct approximations are taken; however, the interpretation of quantum mechanics gives a different philosophical and physical description of nature.

Young's experiment has been used as a way to interpret quantum mechanics as a probabilistic description, Copenhagen interpretation. Bearing this in mind, the interference pattern observed classically and quantum mechanically is generated by the arrival of many photons at different places and with different probabilities. In textbooks, most of the time, one can usually find only the simple case scenario, in which the interference pattern is generated by the arrival of one photon at a time [6]. Now we know that this is an approximation limited by the way the source and the detection process are treated. We have used Fock and coherent states together with multi-photon counting apparatus, to observe the differences between classical and quantum interferometry.

Developments in experimental physics have taken advantage of the quantum description of light to extract information from the system under study, or to construct different quantum states. These experiments require a more realistic description of a photon source, which cannot be considered to be like a photon gun, emitting one photon a time. We know that higher order photon numbers are required to describe a more realistic source, such as the laser. This description of light can be used to understand the new physics, and has been the focus in the development of areas such as quantum optics, quantum information [7,8], quantum imaging [9,10], and quantum lithography [11]. For example, having a multi-particle state in a coherent superposition will give non local interaction between multi-particles. Such non-local interactions were described by Einstein as "spooky action at a distance". The resulting states generated by a superposition of multi-particle states leads to a non-separable state known as entangled state [12]. Entanglement is a pure quantum mechanical phenomenon, and has been at the heart of many areas of research, *i.e.* quantum teleportation, a technique used to transfer a quantum state from one place to another.

Quantum optics has been very fruitful area of research, where several experiments have reported on the preparation and use of multi-photon states that show non-local effects. In the area of quantum interferometry, several experiments have used entangled states as a way to exceed the classical Rayleigh diffraction limit. This is accomplished by using entangled states to show an effective de Broglie wavelength that is inversely proportional to the number of photons in the state of the system [13]. One way to achieve this is to consider entangled states of three and four photons produced by spontaneous parametric down conversion (SPDC) [14], and the performance of coincidence detection of the states can in fact exceed the diffraction limit by a factor n corresponding to the number of entangled photons used [15,16].

Another exciting interferometric experiment is known as "ghost imaging" [17]. In this case, an entangled state (signal and idler) is formed by SPDC; the signal photon propagates through a double slit, and the idler propagates freely following two different optical paths. When coincidence detection and position correlations are analyzed, the image and the interference pattern of the double slit are reconstructed. This imaging technique needs to satisfy EPR inequalities and has raised some controversy. Some authors have argued that the correlation between states in "ghost imaging" are classical and not quantum in nature [18]. However, it was been shown that the quantum correlations of any sources of classically correlated pairs of quanta can never achieve a perfect correlation of both momentum and position variables, as expected in the case of entanglement [19].

Most, if not all, of the cases briefly mentioned above use higher-order correlation analysis as a way to surpass the diffraction limit. We present the use of the most basic quantum interferometry scheme, Young's experiment, described in terms of operator notation to introduce basic notions of quantum interferometry, and to show how entanglement and an adequate selection of the measurement apparatus can overcome the classical Rayleigh diffraction limit. For this reason we start the discussion of the topic, Section 2, with a brief description of the classical Young's experiment. This is followed, Sec. 3, by a description of the quantum Young's experiment where two kinds of initial states of the boson field are considered —Fock and coherent states—, and a photon counter operator is used to describe the measurement process. Results are presented and discussed next, Sec. 4, showing that an effective de Broglie wavelength is obtained which is inversely proportional to the number of photons in the source if and only if the photon counter can resolve that specific number of photons. Finally, we close in Sec. 5, with a discussion on the relationship of our work with the more complicated schemes of today's research.

2. Classical Young's experiment

Young's experiment, executed at the beginning of the 1800's and considered to be a model for researchers today, was the first scheme to demonstrate the interference of light [20]. In the modern version of this experiment, a monochromatic electromagnetic plane wave impinges on a screen, Young's screen, with two pinholes that are close together. Away from and parallel to Young's screen, there is a detection plane — which will be called the detection screen— where an interference pattern is formed[ii]. The experiment can be generalized to a multi-pinhole scheme. Figure 1 presents a diagram of the multi-pinhole Young's experiment.

Mathematically, each and every pinhole in the Young's screen can be described as a point source of spherical waves with a common phase. For simplicity, this common phase is assumed to be zero. Therefore, the electromagnetic field at a point x at a given time on the detection plane is given by the superposition

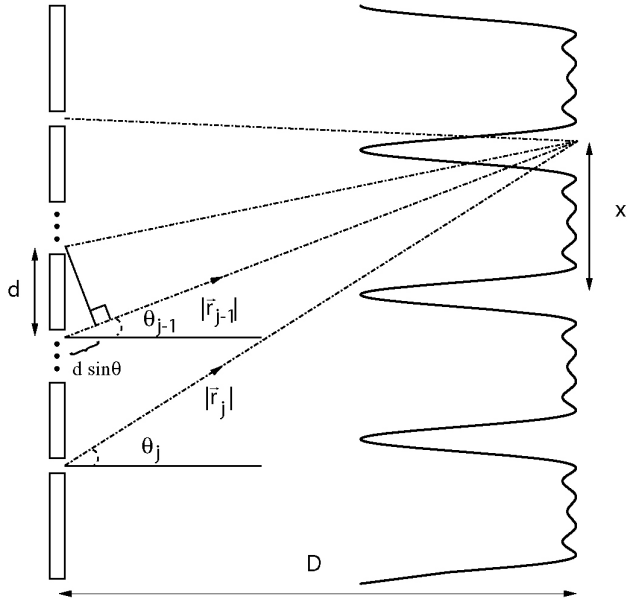

FIGURE 1. Schematic diagram for a multi-slit Young's experiment.

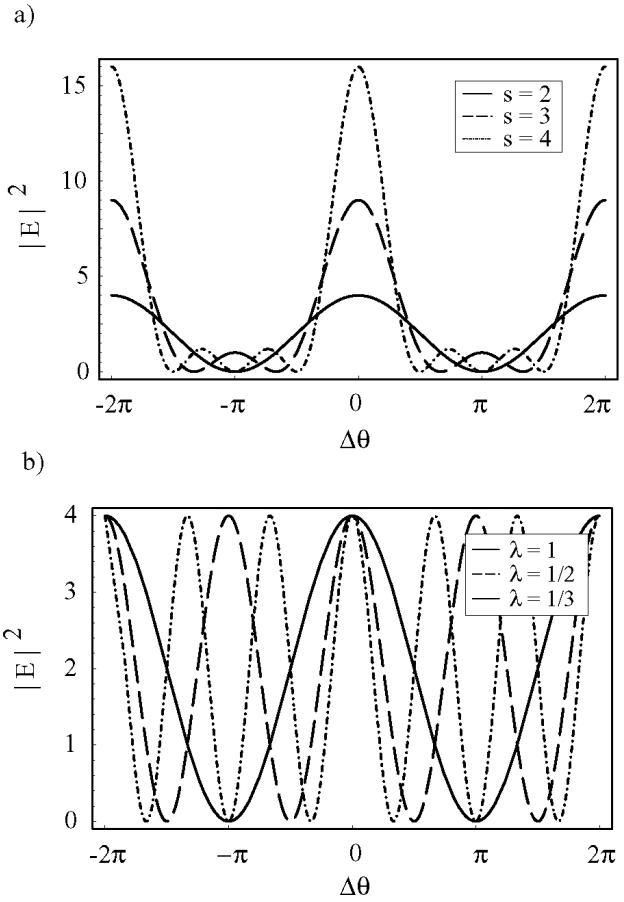

FIGURE 2. Classical results of Young's experiment of unnormalized intensity, $\langle I\rangle$ a.u., on the detection screen versus the parameter $\Delta\theta$, in units of λ. Panel a) shows the case in which Young's screen has a different number of pinholes, $s = 2$ solid line, $s = 3$ dashed line, $s = 4$ dotted line. Panel b) represents the case of a double slit ($s = 2$) for $\lambda = 1$ solid line, $\lambda = 1/2$ dashed line, $\lambda = 1/3$ dotted line.

$$E(x) = \sum_{j=1}^{s} A_j e^{-\imath 2\pi|\vec{r}_j|/\lambda}, \tag{1}$$

where the quantity s is the total number of pinholes, A_j is the amplitude of the field for the j-th pinhole, and $|\vec{r}_j|$ is the distance from the j-th pinhole to the point x. The quantity λ is the wavelength of the impinging light.

Assuming equidistant pinholes with equal transmittance, and using a shorthand notation of $\theta_j = 2\pi|\vec{r}_j|/\lambda$, the intensity of the field at a point x on the detection plane is given by the equation

$$\begin{aligned} I(x) &= |E(x)|^2, \\ &= |A|^2 \sum_{j,k=1}^{s} e^{-\imath(j-k)\Delta\theta}, \\ &= |A|^2 \left[s + 2\sum_{j=1}^{s-1} (s-j)\cos j\Delta\theta \right]. \end{aligned} \tag{2}$$

We have used the geometry of the problem to define $(j-k)\Delta\theta = \theta_j - \theta_k$, using the fact that the detection screen distance from Young's screen, D, is larger than the equidistant separation of pinholes, d. With these conditions, one can find, for the double slit case, the maximum constructive interference when $d\sin\theta = l\lambda$, where l is the order of the interference ($l = 0, \pm1, \pm2, \ldots$). Straightforward calculation gives interference fringes as shown in Fig. 2 for a different number of pinholes.

One can appreciate that, even though multiple oscillations appear when the number of pinholes is larger than two, $s > 2$, the separation between the interference maxima is given by the wavelength used in the experiment. The Rayleigh criterion states that the minimum resolvable separation by a diffractive system is proportional to $\lambda/2$.

Figure 2 shows the effects on the interference pattern when $s = 2, 3, 4$ (panel a). Another example (panel b) is the case for a double slit for $\lambda = 1, 1/2, 1/3$. We can observe that the number of fringes increases with a smaller wavelength. This is the well-known classic result. Panel b in Fig. 2 will become important for explaining the results obtained for the quantum analog of Young's experiment.

3. Quantum Young's Experiment

We can use Feynman's words [21] to describe the importance of Young's experiment: "[it] has in it the heart of quantum mechanics". Therefore, to fully describe the phenomenon observed since the beginning of the 1800's, we need to introduce the quantum properties of light.

The mathematical analysis of Young's experiment is done by considering the quantization of an electromagnetic field in a limited volume of space situated between the photon source and the detection screen; the s-slit Young's screen is located somewhere in between the two. Without Young's screen, the mathematical analysis reduces to a calculation of the quantization of the electromagnetic field in a cavity, which is solved by using Fock states or coherent states, and can be found in several textbooks [4-6]. This quantization is written as a traveling wave with periodical boundary conditions associated with the source/detector pairs, and could be expressed as a quantum harmonic oscillator with eigenvalues,

$$E_n = \hbar\omega\left(n + \frac{1}{2}\right), \tag{3}$$

where the n-th state has n quantum of energy and frequency ω. Each quantum of energy is called a photon. The probability amplitude of finding an n-quantum state (n-photon state or Fock state $|n\rangle$) in a position state ($|x\rangle$), for the one-dimensional case, is expressed in terms of the Hermite polynomials [$H_n(x) = (-1)^n e^{x^2}(d^n/dx^n)e^{-x^2}$] as,

$$\begin{aligned} \langle x|n\rangle = \frac{1}{\sqrt{2^n n!}} \left(\frac{m\omega}{\pi\hbar}\right)^{\frac{1}{4}} \exp\left(-\frac{m\omega x^2}{2\hbar}\right) \\ \times H_n\left(\sqrt{\frac{m\omega}{\hbar}}x\right). \end{aligned} \tag{4}$$

This equation represents the delocalization in the space of what we know as photons. Thus, in order to understand the principle behind the quantum nature of Young's experiment, we divide the whole process into four parts: the photon source, the Young's screen, the free propagation stage, and the detection screen. In the following subsections we will describe the four stages and describe a series of assumptions that we have employed to understand quantum interferometry using an operator approach[iii].

3.1. Photon source

The role of the photon source in Young's experiment must be understood by having in mind that there is a propagation time t between the emitting source and the detection screen. When we talk about the detection of photons (Sec. 3.4) we consider that the photons are captured by a detection screen. A simple approach is to consider that photons follow a ballistic trajectory from the source to the detector. This physical idealization for photons is easier to grasp. In other words, we are considering the photon source as a photon gun. However, one must be very careful because, by doing so, one could be misled into believing in a localized description of the photon, which is not physically appropriate. With the photon gun assumption, we are going to have s-propagation modes defined by each of the slits. And, since we do not know the path that the photon will follow, we need to consider all possible trajectories; we will not allow the break-up of the state, but it will reach the detector at some fixed point in the detection screen, as will be shown below. Under this scheme, the photon source can be described by a quantized monochromatic electromagnetic field inside a single-mode cavity, which is written as a series of eigenstates. One of those eigenstates is known as Fock—or number—states:

$$|\psi_0\rangle = |n\rangle, \tag{5}$$

where n is an integer. A Fock state of the electromagnetic field is represented with a well-defined number of photons in it, n photons for state $|n\rangle$ [22]. Another of these eigenstates are the coherent states:

$$|\psi_0\rangle = |\alpha\rangle = e^{-|\alpha|^2/2} \sum_{n=0}^{\infty} \frac{\alpha^n}{\sqrt{n!}} |n\rangle. \tag{6}$$

A coherent state, introduced by Glauber [23], is a superposition of Fock states with a Poisson distribution; they are a good approximation of the light produced by an ideal laser.

Being rigorous, we should consider for a traveling wave packet of photons some spatial distribution of a multi-mode state of the field described by

$$|\psi(\vec{r},t)\rangle = \sum_{j=1}^{k} f(\vec{r},t)|\psi_0\rangle_j. \tag{7}$$

This description will lead to additional operations in all the treatments below. For simplicity, we shall consider only one mode of the field, treating the states as given in Eqs. 5 and 6 as the outgoing states of the source and into Young's experiment, even when they are not wave packets in any rigorous sense.

3.2. Young's screen

Young's screen can be seen as a mode plexing device. The above described states of the field are transformed into a coherent superposition of multi-mode Fock or Coherent states after impinging on the Young's screen and going through the pinholes. The Young's screen acts as a maximal entangler for this case, due to the bosonic properties of photons [6]. A Fock or coherent state impinging on the Young's screen will go through one and only one of the pinholes; each pinhole defines a mode of transmission for the electromagnetic field; each mode has an equal opportunity of being populated by the impinging state. In other words, the initial state with many photons will not break apart and follow multiple paths. The state after the Young's screen can be written as:

$$|\psi_Y\rangle = \frac{1}{\sqrt{s}} \sum_{j=1}^{s} |\psi_{n,j}\rangle, \tag{8}$$

for an initial Fock state, where the state $|\psi_{n,j}\rangle$ represents the initial Fock state $|n\rangle$ going through the j-th pinhole and the vacuum state, $|0\rangle$, going through the other $j-1$ pinholes. Or, for a coherent initial state:

$$|\psi_Y\rangle = \frac{1}{\sqrt{s}} \sum_{j=1}^{s} |\psi_{\alpha,j}\rangle, \tag{9}$$

where the state $|\psi_{\alpha,j}\rangle$ corresponds to the initial coherent state $|\alpha\rangle$ that followed the path through the j-th pinhole, and there are no photons going through the other $j-1$ pinholes. These states, Eqs. (8) and (9), are called maximal entangled states.

Furthermore, something that we must remember is that Young's screen defines the transmission modes just by being there. The transmission modes are the possible paths that the photon package can take. With a photon source that only allows a photon package to be inside the experiment at a certain time, it would be impossible to break up the incoming state. A similar effect is produced by the presence of a beam splitter. In this case the beam splitter functions as an amplitude splitting device, so that conceptually it is different from the Young's screen, in which the transmission is defined by the possible path of the wavefront. Even though both experiments serve to describe interference, quantum mechanically they interact with the quantum state in different ways. In the quantum regime, a beam splitter is a two-mode input and two-mode output that couples two harmonic oscillator modes and they can "break up" or "add up" photon states. The beam splitter is an "active device", while Young's screen is a "passive device", defining transmission modes by defining transmission paths, and coupling the existing state with a vacuum state.

Having stated the difference between the classical and quantum perspectives, a quantum Young's screen and a quantum beamsplitter agree in some situations. For example, if we consider that there is one photon in each input port of a 50/50 beamsplitter, then the output will be $|20\rangle + |02\rangle$ (up to some normalization and phase factor), which means we have an equal chance of having both photons coming out of one of the output ports, and the other port being left alone. In this case, it can be compared to having a two-photon state impinging on a Young's screen. We conclude that, at least in the cases of (a) one photon through one input port of a 50/50 beamsplitter and no photon through the other, and (b) one photon in each input port of a 50/50 beamsplitter, the outputs of Young's screen and a Beam Splitter can be considered equal, with (a) one photon impinging on the screen, (b) two photons impinging on the screen. From this reasoning we consider that an m-slit Young's screen can be seen as a kind of equal probability multiplexing device that does not break up the incoming state.

3.3. Free propagation

After the interaction with Young's screen, the state of the system evolves through free space. This free space evolution can be described by the evolution operator [22]:

$$\hat{U} = e^{-\imath\hat{\xi}}, \qquad \hat{\xi} = \sum_{j=1}^{n} \theta_j \hat{n}_j, \tag{10}$$

where the operator $\hat{n}_j$ is the bosonic number operator for the j-th transmission mode, and $\theta_j = 2\pi|\vec{r}_j(x)|/\lambda$, as shown in Fig. 1. The quantity λ is the wavelength of the photon source used. The evolution operator in Eq. (10) will introduce a phase shift dependent on the path taken by the state of the field. It is important to remember that this approximation for θ is only valid when the distance between the Young's screen and the detection screen is greater than the separation between pinholes ($D \gg d$), as in the classical case.

With the evolution operator as described in Eq. (10), we can write the state of the system as it impinges the detection screen as:

$$|\psi_D\rangle = \hat{U}|\psi_Y\rangle. \tag{11}$$

3.4. Detection screen

Up to this point in our description, classical and quantum versions of Young's experiment both have been dealing with the propagation of a state of the light after impinging on a Young's screen. The two cases are not significantly different, but special states of light were considered in the quantum case.

Another difference from the classical case is introduced by considering not a simple "click on photon arrival" detector, but a "click when m-photons arrive" detector, an m-photon detector. In the Appendix, the photon counting of one photon at a time is described, and a number operator is defined in Eq. (A.11). The properties of such an operator are presented. For our purposes, we use an m-photon detector that leads to the mean m-photon counts described by:

$$\langle M\rangle = \langle\psi_D|\hat{A}^{\dagger m}\hat{A^m}|\psi_D\rangle. \tag{12}$$

In the next section, both cases for an initial state consisting of Fock or Coherent states will be dealt with.

4. Results on quantum interferometry

4.1. Fock states interferometry

Using Fock states as initial states [Eq. (5)], the probability of having a detection event at the point x in the detection screen is given by:

$$\langle M\rangle = \frac{1}{s}\sum_{j,k=1}^{s}\langle\psi_{n,j}|\hat{U}^\dagger\hat{A}^{\dagger m}\hat{A^m}\hat{U}|\psi_{n,j}\rangle, \tag{13}$$

which can be separated into three different cases according to the number of photons in the Fock state, n, and the number of photons the measurement apparatus resolves, m:

- $n < m$,
$$\langle M\rangle = 0. \tag{14}$$
- $n = m$,
$$\langle M\rangle = \frac{n!}{s}\sum_{j,k=1}^{s} e^{-\imath\, n(j-k)\Delta\theta} = \frac{n!}{s}\left[s + 2\sum_{j=1}^{s-1}(s-j)\cos(jn\Delta\theta)\right]. \tag{15}$$
- $n > m$,
$$\langle M\rangle = \sqrt{\frac{n!}{(n-m)!}}. \tag{16}$$

These equations, Eq. (14)-(16), show that just the right combination of an n-photon source with an m-photon detection screen results in a interference-like pattern when considering the probability of an m-photon detection to happen at the point x on the detection screen:

$$\langle M\rangle = \frac{m!}{s}\left[s + 2\sum_{j=1}^{s-1}(s-j)\cos(jm\Delta\theta)\right]. \tag{17}$$

Figure 3 shows some possible outcomes of Eq. (15). In panel a), the classical result is obtained when a one-photon source and a one-photon detector are used for different numbers of pinholes. We note that Figs. 3a and 2a are equivalent; now Fig. 2a represents the arrival and detection of one photon at a time. However, the important result comes from considering higher-order detection processes, $n = m$, $m > 1$. In this condition, the probability of a detection event has a distribution that depends on the number of photons, m. Panel b) shows, that using two slits, as the number of photon detection

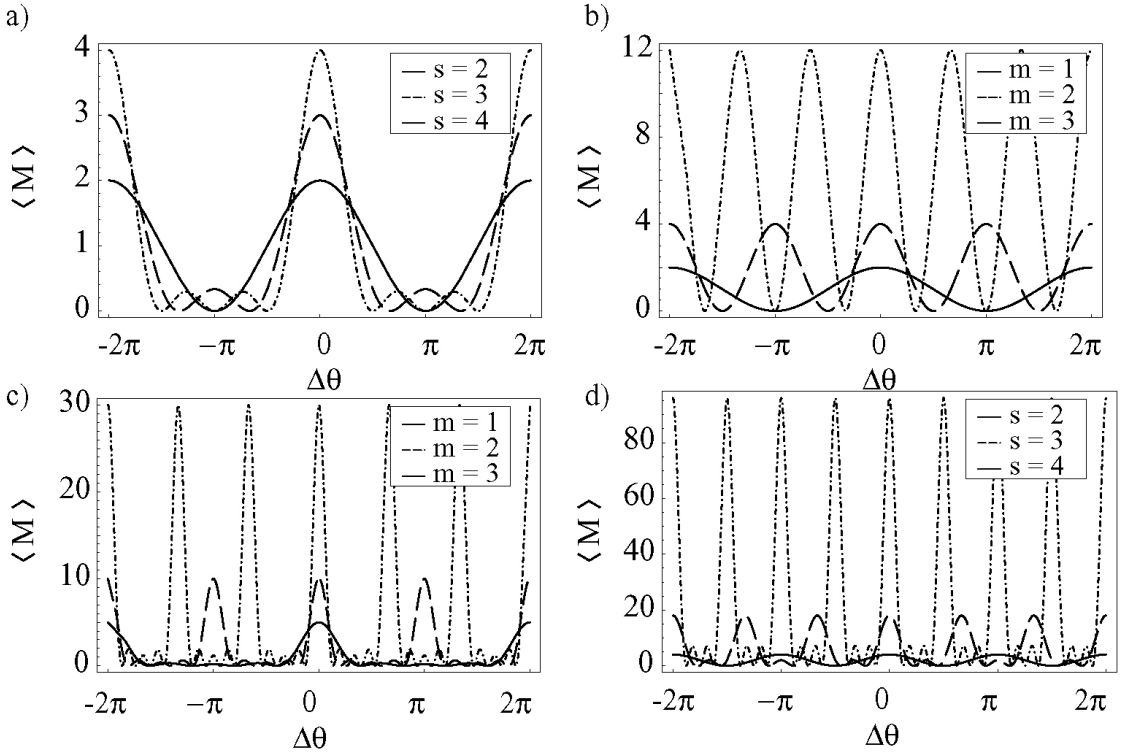

FIGURE 3. Un-normalized quantum interferometry using Fock states as the source and multi-photon detector. Panel a) shows the classical result, n=m=1. Panel b) presents the case when $n = m$ for the particular case of two-slits, $s = 2$. In panel c) we observe the effects for the case of five slits, and in panel d) we present the case when the number of slits is the same as the photon detection process, which is used only for illustrating various interference patterns.

increases, the number of fringes increases, and the distance between two interference maxima is reduced by a factor m. This is equivalent to considering an effective de Broglie wavelength that is inversely proportional to the number of photons used, $\lambda_{eff} = \lambda/m$, which means that it is possible to surpass the Rayleigh diffraction limit by the same factor m. Panel c) presents behavior similar to that in panel b), but for a situation with five slits. And finally, panel d) shows a case where $m = s$ as a way to present different patterns obtained as one increases the number of pinholes used in the experiment.

4.2. Coherent states interferometry

Using as the initial state a coherent state, Eq. 6, and the results for Fock states interferometry presented above, it is possible to calculate the probability of a detection event at the point x on the detection screen as:

$$\langle M\rangle = e^{-|\alpha|^2}\sum_{n,m=0}^{\infty}\frac{\alpha^{\star n}\alpha^m}{\sqrt{n!m!}}\langle n|\hat{U}^\dagger\hat{A}^{\dagger\,m}\hat{A}^m\hat{U}|m\rangle,$$

$$= e^{-|\alpha|^2}\left\{\frac{m!}{s}\left[s + 2\sum_{j=1}^{s-1}(s-j)\cos(j\,m\Delta\theta)\right]\right\}. \quad (18)$$

In Eq. (18), an interference term dependent on the m-photon detector—first RHS term—and a bias term—second RHS term—are found. Again, a distribution of the probability of a detection event similar to the classical term is obtained when the photon counter is set for $m = 1$, and an effective de Broglie wavelength $\lambda_{eff} = \lambda/m$ is observed when the photon counter is set for $m \geq 1$. But the resolution of the interference fringes diminishes as the expectation value for the number operator of coherent states increases: $\langle n\rangle = |\alpha|^2$. This is due to the bias term.

Equation (18) is almost identical to Eq. (17) except for the factor corresponding to an exponential decay in α. This effect is shown in Fig. 4 for different values of α, ranging

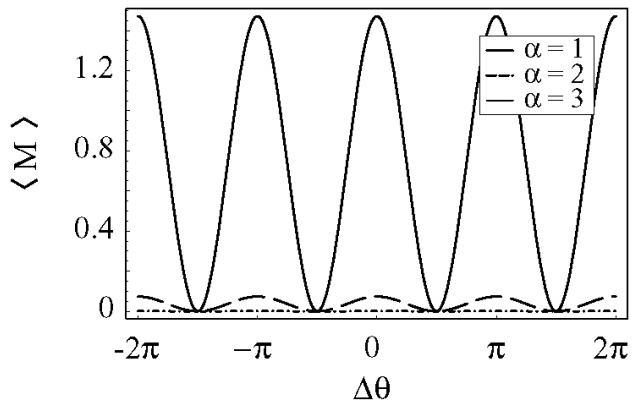

FIGURE 4. Quantum interference of a double slit using a two photon detection process with coherent state for $\alpha = 1, 2, 3$.

from 1 to 3. In this particular case, we considered a double-slit ($s = 2$), a two photon detection process($m = 2$), and coherent states. It is clear that the contrast decreases as the α increase. At that moment we loose the ability to observe any interference.

5. Conclusion

We have presented a simple yet descriptive operator-based approach to a generalized Young's experiment. The results show that the use of an m-photon source and counting detection scheme produces a modification in the modulation of the interference pattern, giving an effective de Broglie wavelength of:

$$\lambda_{eff} = \lambda/m. \tag{19}$$

This is the heart of quantum interferometry; basically, the interference pattern observed is a function of the number state of the source and the detection process, as stated in the introduction and observed in our results. From quantum mechanics, this could be accomplished by higher order correlations or using higher order photon detection processes. However, both methods use the quantum properties of light to describe interference not as a superposition of electromagnetic waves, but as the spatial probability in the detection or correlations in the detection of the photon states. When quantum states are used, the interference pattern observed has the signature of an effective de Broglie wavelength [Eq. (19)].

Advances in new photon detectors, especially the case of VLPC, have made it possible to observe higher order quantum interferometry [24]. This particular detector was developed for a particle tracking system [25]. It could be used as the photon counting device required to observe the interferometry fringes predicted by quantum analysis. The operation of a VLPC is similar to an avalanche photodiode; in this case the number of absorbed photons in a light pulse is obtained by measuring the height of the current pulse from the detector [26]. One can take advantage of this technology and do higher order quantum interferometry.

A proposed experimental set-up would require a highly attenuated laser where the mean value of photons could be considered small. The light from this source should impinge on a double slit. Finally, with a VLPC, the photon states would be detected using the height of the current from the detector; this could be done for each of the number of photons states. One will be able to observe the quantum interference described here by scanning the detector parallel to the Young's screen.

The authors realize that in this operator-based study of Young's experiment, they have used a very simple application, since for the analysis they have not considered proper wave packets. But taking into consideration proper wave-packets would involve more confusing procedures and obscure the main point. This said, consider our presentation for the sake of showing the result of surpassing the Rayleigh diffraction limit using quantum interferometry. For an advanced theoretical discussion of position representation, we recommend reading [27,28].

As a final note, for practical applications of a scheme such as the one presented here —*e.g.* quantum lithography— it would be necessary to have n-photon sources along with materials which are m-photon absorbers, in order to exploit this theoretical prediction to surpass the Rayleigh diffraction limit. As results show, even the use of materials that are m-photon absorbers with coherent-like states of light would lead to poor resolution if the mean photon number were large. Another important fact to consider in quantum lithography is the contrast between fringes. Thus, there is no need to have a better resolution if the contrast is lost. Some of current state-of-the-art research is directed towards using the quantum properties of light to create better and smaller electronic chips by increasing resolution and contrast [9].

Another approach is to take advantage not only of these higher-order effects but also of higher order correlations in space and frequency, and apply them to microscopy [10]. This effort is driven by the fact that an increasingly better and higher resolution is required to study how molecules move and interact *in vivo*. Other methods that do not use these higher-order correlations have been implemented in microscopy that exceeds the classical limit of diffraction [29,30]. However, such effects do not use the quantum properties of light as the basic mechanism for improving resolution.

Appendix: Photon Detection

It is well known that, experimentally, the detection process happens via photon absorption by different means. Most commonly, this process is realized by photo-ionization. This means that the electric field associated with this process is the one that is measured. For this purpose it is convenient to start with a definition of the complex electric field operator that is obtained from the field quantization. The electric field operator $\hat{E}(\mathbf{x}, t)$ consists of two parts that could be shown explicitly with time- and space- dependence:

$$\hat{E}(\mathbf{x}, t) = \hat{E}^{(+)}(\mathbf{x}, t) + \hat{E}^{(-)}(\mathbf{x}, t). \tag{A.1}$$

Each of the components can be represented as a function of the creation $\hat{a}^\dagger$ and annihilation $\hat{a}$ operators like

$$\hat{E}^{(+)}(\mathbf{x}, t) = \imath \sum_k \left(\frac{\hbar\omega_k}{2\epsilon_0 V} \right)^{1/2} \varepsilon_k \hat{a}_k \times \exp(-\imath\omega_k t + \imath \mathbf{k}\cdot\mathbf{x}), \tag{A.2}$$

with a complex conjugate described by

$$\hat{E}^{(-)}(\mathbf{x}, t) = -\imath \sum_k \left(\frac{\hbar\omega_k}{2\epsilon_0 V} \right)^{1/2} \varepsilon_k \hat{a}_k^\dagger \times \exp(\imath\omega_k t - \imath \mathbf{k}\cdot\mathbf{x}). \tag{A.3}$$

Such operators need to satisfy the following:

$$\hat{E}^{(+)}(\mathbf{x},t)|0\rangle = 0, \tag{A.4}$$

$$\langle 0|\hat{E}^{(-)}(\mathbf{x},t) = 0. \tag{A.5}$$

In other words, the process of absorption or annihilation in the vacuum state is null.

In the real world, a photographic plate or a photomultiplier tube (PMT) absorbs one or more photons. This process can be explained by the photoelectric effect. For a PMT, the absorption of a photon by an atom causes excitation of an electron from a bound state to a free state in which it can be released from the atom altogether. However, one can describe these transitions made by the electric field at detection, without going into the details of how radiation interacts with matter. For example, if one considers an ideal photon detector that is frequency-independent, one can write the probability of transitions from an initial state to $|\Psi_i\rangle$ to a final state $|\Psi_f\rangle$ as the sum of all the transitions squared:

$$\sum_f |\langle\Psi_f|\hat{E}^{(+)}(\mathbf{x},t)|\Psi_i\rangle|^2 = \langle\Psi_i|\hat{E}^{(-)}(\mathbf{x},t)\hat{E}^{(+)}(\mathbf{x},t)|\Psi_i\rangle. \tag{A.6}$$

A simpler way to write this is to consider an operator $\hat{N}$, sometimes called intensity operator, as a function of the creation and annihilation operators like

$$\hat{N} = \hat{E}^{(-)}(\mathbf{x},t)\hat{E}^{(+)}(\mathbf{x},t), \tag{A.7}$$

$$\propto \hat{a}^\dagger\hat{a}, \tag{A.8}$$

such that when averaged it gives the number of photons detected by the process described above.

In the generalized Young's experiment, the screen could be thought of as a multiplexor, where the initial state is divided into multiple modes, j, each of which has corresponding annihilation ($\hat{A}$) and creation operators ($\hat{A}^\dagger$). Thus, one could define an operator $\hat{A}$ that corresponds to the sum of all the annihilation operators of each of the nodes of the field and were written

$$\hat{A} = \sum_{j=1}^{s}\hat{a}_j, \tag{A.9}$$

where the operator $\hat{a}_j$ is the annihilation operator for the j-th node. Similarly the complex conjugate is defined as

$$\hat{A}^\dagger = \sum_{j=1}^{s}\hat{a}_j^\dagger. \tag{A.10}$$

A number operator can similarly be defined by the multiplication of the previous two equations

$$\hat{N} = \hat{A}^\dagger\hat{A}. \tag{A.11}$$

The properties of the previously defined operators is summarized in the commutation relationships given by

$$[\hat{A},\hat{A}^\dagger] = \sum_{j=1}^{s}[\hat{a}_j,\hat{a}_j^\dagger] = -s, \tag{A.12}$$

$$[\hat{A}^\dagger,\hat{A}] = \sum_{j=1}^{s}[\hat{a}_j^\dagger,\hat{a}_j] = s, \tag{A.13}$$

$$[\hat{N},\hat{A}] = [\hat{A}^\dagger,\hat{A}]\hat{A}, \tag{A.15}$$

$$[\hat{N},\hat{A}^\dagger] = \hat{A}^\dagger[\hat{A},\hat{A}^\dagger]. \tag{A.16}$$

When such operators interact with the states of the system, they do so in the following way:

$$\hat{A}|\psi_{Y,n,s}\rangle = \sqrt{n}|\psi_{Y,n-1,s}\rangle, \tag{A.17}$$

$$\hat{A}^\dagger|\psi_{Y,n,s}\rangle = \sqrt{n+1}|\psi_{Y,n+1,s}\rangle, \tag{A.18}$$

$$\hat{N}|\psi_{Y,n,s}\rangle = n|\psi_{Y,n,s}\rangle \tag{A.19}$$

It is clear to see that

$$\hat{A}^m|\psi_{Y,n,s}\rangle = \sqrt{\frac{n!}{(n-m)!}}|\psi_{Y,n-m,s}\rangle,\ n \geq m \tag{A.20}$$

$$\hat{A}^{\dagger m}|\psi_{Y,n,s}\rangle = \sqrt{\frac{(n+m)!}{n!}}|\psi_{Y,n+m,s}\rangle, \tag{A.21}$$

One can compute the temporal evolution of the annihilation operator given by:

$$\hat{A}(t) = \hat{U}^\dagger(t)\hat{A}\hat{U}(t), \tag{A.22}$$

using all the geometric considerations exposed in the main part of this letter—as:

$$\begin{aligned}\hat{A}(t) &= e^{\imath\sum_j\theta_j\hat{n}_j}\ \sum_k \hat{a}_k\ e^{-\imath\sum_l\theta_l\hat{n}_l},\\ &= \sum_{j=1}^{s} e^{\imath\theta_j\hat{n}_j}\ \hat{a}_j\ e^{-\imath\theta_j\hat{n}_j},\\ &= \sum_{j=1}^{s} e^{\imath\theta_j\hat{n}_j}e^{-\imath\theta_j(\hat{n}_j+1)}\hat{a}_j,\\ &= \sum_{j=1}^{s} e^{-\imath\theta_j}\hat{a}_j,\\ &= e^{-\imath\theta_1}\sum_{j=1}^{s} e^{-\imath(j-1)\Delta\theta}\hat{a}_j,\end{aligned} \tag{A.23}$$

where we have defined $\Delta\theta = \theta_n - \theta_{n-1}$, thanks to the geometry of the problem. The same can be done for the adjoint of $\hat{A}$, or creation operator.

Finally, for multiphoton detection, the detection process is given by the simultaneous annihilation of m-photons or $\hat{A}^m$ such that one can define an m-photon counter, $\hat{M}$, which "click as m-photons arrive":

$$\hat{M} = \hat{A}^{\dagger\, m}\hat{A}^m = \left(e^{\imath\theta_1}\sum_{j=1}^{s} e^{\imath(j-1)\Delta\theta}\hat{a}_j^\dagger\right)^m \left(e^{-\imath\theta_1}\sum_{k=1}^{s} e^{-\imath(k-1)\Delta\theta}\hat{a}_k\right)^m \tag{A.24}$$

$$= \left(\sum_{j=1}^{s} e^{\imath(j-1)\Delta\theta}\hat{a}_j^\dagger\right)^m \left(\sum_{k=1}^{s} e^{-\imath(k-1)\Delta\theta}\hat{a}_k\right)^m . \tag{A.25}$$

The time evolution of this operator can be easily calculated from Eq. (A.23).

---

i For a current review on understanding what a photon is, we suggest Ref. 3.

ii For a graphic description of this topic we recommend the reader to look at the following on-line trailer, http://www.whatthebleep.com/trailer/doubleslit.wm.low.html.

iii Most of the assumptions used are presented with the sole purpose of clarifying the concepts that will give rise to an effective de Broglie wavelength that surpasses the Rayleigh classical limit of diffraction.

1. M. Born and E. Wolf, *Principles of Optics: Eledtromagnetic Theoty of Propagation, Interference and Diffracton of Light*, 7th ed. (Cambridge University Press, 1999).
2. K.T. Hecht, *Quantum Mechanics* (Springer, 2005).
3. C. Roychoudhuri and R. Roy, *Opt. Photonics News* **14** (2003) S1.
4. M.O. Scully and M.S. Zubairy, *Quantum optics*, 1st ed. (Cambridge Universite, Press, Cambridge, 1997).
5. P. Meystre and M. Sargent III, *Elements of quantum optics*, 3rd ed. (Springer-Verlag, Berlin, 1998).
6. R. Loudon, *The quantum theory of light*, 2nd ed. (Oxford University Press, 1983).
7. M. Nielsen and I. Chuang, *Quantum Computation and Quantum Communication* (Cambridge Univ. Press, 2000).
8. D. Bowmeester and A. Zeilinger, The physics of quantum information: quantum cryptography, quantum teleportation, quantum computation (Springer-Verlag, Berlin, 2000).
9. A. Muthukrishnan, M. Scully, and M. Zubairy, *J. Opt. B* **6** (2004) S575.
10. G. Bjork, J. Soderholm, and L.L. Sanchez-Soto, *J. Opt. Soc. Am. B* **6** (2004) S478.
11. A. Boto *et al.*, *Phys. Rev. Lett.* **85** (2000) 2733.
12. A. Zeilinger, *Rev. Mod. Phys.* **71** (1999) 288.
13. E. Fonseca, P. Souto Ribeiro, A. Pádua, and C. Monken, *Phys. Rev. A* **60** (1999) 1530.
14. J. Perina, B. Saleh, and M. Teich, *Rev. Rev. A* **49** (1998) 3972.
15. M. Mitchell, J. Lundeen, and A Steinberg, *Nature* **429** (2004) 161.
16. P. Walther *et al.*, *Nature* **429** (2004) 158.
17. M. D'Angelo, M. Chekhova, and Y. Shih, *Phys. Rev. Lett.* **87** (2001) 013602.
18. R. Bennink, S. Bentley, and R. Boyd, *Phys. Rev. Lett.* **89** (2002) 113601.
19. M. D'Angelo, Y.-H. Kim, S.P. Kulik, and Y. Shih, *Phys. Rev. Lett.* **92** (2004) 233601.
20. M. Born and E. Wolf, Principles of optics (Cambridge University Press, Cambridge, 1999).
21. R.P. Feynman, R.B. Leighton, and M. Sands, The Feyman lectures on physics III: quantum mechanics (Addison-Wesley, Massachusetts, 1965).
22. L. Allen and J. Eberly, *Optical resonace and two-level atoms* (Wyley, New York, 1975).
23. R. Glauber, *Phys. Rev.* **130** (1963) 2529.
24. J. Kim, S. Takeuchi, and Y. Yamamoto, *Appl. Phys. Lett.* **74** (1999) 902.
25. D. Lincoln, *Nucl. Inst. Meth. A* **453** (2000) 177.
26. G. Khouty, H. Eisenberg, E. Fonseca, and D. Bouwmeester, quant-ph/0601104 p. 0601104 (2006).
27. E.R. Floyd, quant-ph/0605120 (2006).
28. E.R. Floyd, quant-ph/0605121 (2006).
29. S.W. Hell, *Nat. Biotechnol.* **21** (2003) 1347.
30. M.G.L. Gustasfsson, *J. Microsc.* **298** (2000) 82.